BULLETIN OF THE POLISH ACADEMY OF SCIENCES
TECHNICAL SCIENCES, Vol. 69(4), 2021, Article number: e137508
DOI: 10.24425/bpasts.2021.137508

Identification of longitudinal aerodynamic characteristics of a strake-wing micro aerial vehicle by using artificial neural networks

Dariusz RYKACZEWSKI[1], Mirosław NOWAKOWSKI[1], Krzysztof SIBILSKI[2*], Wiesław WRÓBLEWSKI[3], and Michał GARBOWSKI[4]

[1] Air Force Institute of Technology, ul. Księcia Bolesława 6, 01-494 Warsaw, Poland
[2] Warsaw University of Technology, Faculty of Power and Aeronautical Engineering, ul. Nowowiejska 24, 00-665 Warsaw, Poland
[3] Wroclaw University of Technology, Faculty Mechanical and Power Engineering, ul. Wyb. Wyspiańskiego 27, 50-370 Wroclaw, Poland
[4] Wroclaw Aircraft Maintenance Services Ltd., ul. Św. Mikołaja 19, 50-062 Wroclaw, Poland

Abstract. Appropriate modeling of unsteady aerodynamic characteristics is required for the study of aircraft dynamics and stability analysis, especially at higher angles of attack. The article presents an example of using artificial neural networks to model such characteristics. The effectiveness of this approach was demonstrated on the example of a strake-wing micro aerial vehicle. The neural model of unsteady aerodynamic characteristics was identified from the dynamic test cycles conducted in a water tunnel. The aerodynamic coefficients were modeled as a function of the flow parameters. The article presents neural models of longitudinal aerodynamic coefficients: lift and pitching moment as functions of angles of attack and reduced frequency. The modeled and trained aerodynamic coefficients show good consistency. This method manifests great potential in the construction of aerodynamic models for flight simulation purposes.

Key words: water tunnel measurements; neural networks; unsteady aerodynamic characteristics; low Reynolds number aerodynamics.

1. INTRODUCTION

Strake-wing micro aerial vehicles (s-wMAV) or micro-aircrafts are a class of autonomous flying robots. Due to their high sensitivity to atmospheric turbulences, it is necessary to develop adequate mathematical models covering wide ranges of flight envelope, including supercritical angles of attack. It is particularly important to develop accurate models of aerodynamics covering a very wide range of operating parameters [1–4].

The article presents an example of the use of artificial neural networks (ANN) to identify the longitudinal aerodynamic characteristics of an s-wMAV. Although this method of identifying aerodynamic characteristics does not give the possibility of obtaining aerodynamic derivatives, it still allows for the identification of time courses and hysteresis of aerodynamic coefficients based on flight tests or dynamic measurements in wind or water tunnels.

Artificial neural networks (ANN) constitute a formal and efficient tool for modeling nonlinear unsteady aerodynamics. The main reason for the successful application of ANN are the universal approximation properties [5], which allow for the use of ANN for any aircraft without significant simplification assumptions. It was found that an NN is able to recreate in real time the histories of unsteady aerodynamic loads [6, 7], using experimental data to train ANN.

*e-mail: krzysztof.sibilski@pw.edu.pl

Manuscript submitted 2021-02-13, revised 2021-05-04, initially accepted for publication 2021-05-11, published in August 2021

2. EXPERIMENTS

Artificial neural networks modeling unstationary aerodynamic characteristics of an s-wMAV have been trained on the basis of test cycles conducted in a water tunnel designed to measure aerodynamic loads on ranges of low Reynolds numbers, angles of attack α, and reduced frequencies f. The reduced frequency f is defined by the following relationship: $f = \omega c_A/V$, where V is light speed or the water tunnel medium flow velocity in [m/s]; c_A is mean aerodynamic chord [m], and ω is an s-wMAV maneuver angular velocity or water tunnel model oscillation angular rate in [1/s].

These tests were carried out in the water tunnel model RHRC 2436 of the Low Reynolds Numbers Aerodynamics Laboratory at the Faculty of Mechanical and Power Engineering of the Wroclaw University of Technology (Fig. 1) [8–10]. The s-wMAV model used for the tests is shown in Fig. 2.

Measurements were carried out under stationary and non-stationary conditions. Aerodynamic characteristics were determined in a wide range of angles of attack and under reduced frequencies of model oscillations in water tunnel measurements of space and slip angles. Due to the position of the strain gauge rigidly related to the tested model in the inclination plane, the values of the lift force were converted from the value of the normal force by projecting the force values onto the plane related to the velocity of the medium flow in the water tunnel. The values of the moment coefficients were converted from the reference point of the aerodynamic balance to the point in MAV model plane of symmetry at 25% of the mean aerodynamic chord. The tests were carried out with

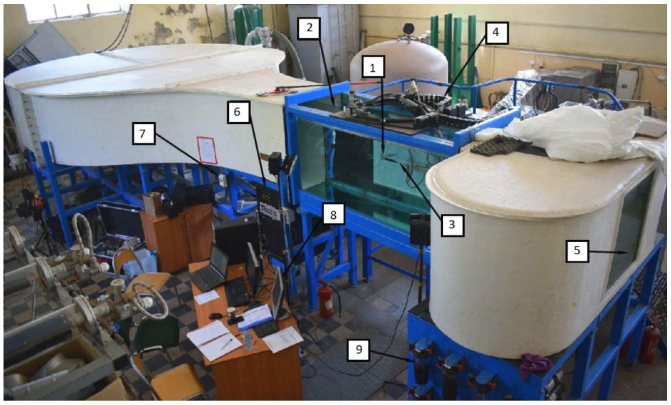

Fig. 1. RHRC 2436 water tunnel in the Nonstationary Aerodynamics Laboratory of the Division of Cryogenic and Aviation Engineering. Overview of the measuring stand: 1 – model in measurements space; 2 – measurement space; 3 – strain gauge (aerodynamic balance); 4 – support; 5 – roll/yaw settings window; 6 – panel of amplifiers; 7 – main switch; 8 – LABVIEW computer station; 9 – system of flow visualization

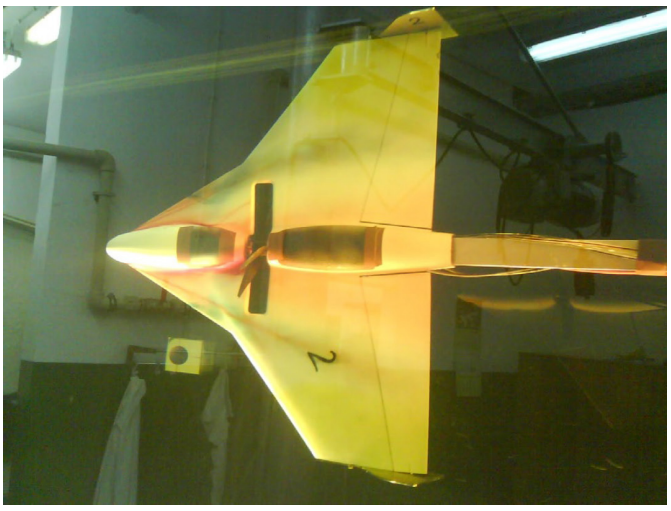

Fig. 2. S-wMAV "Bee" model during tests in a water tunnel

a Reynolds number of 28 000 and have been described in detail in [2, 3].

Figures 3 and 4 show the time courses of the coefficients of the lift force C_Z and the pitching moment C_m. During the tests, the model performed harmonic oscillations in the water tunnel measuring chamber with the amplitude of the angles of attack (pitch angle) $\Delta\alpha = 5^\circ$ around two initial positions angle of attack $\alpha_0 = 25^\circ$ (Fig. 3) and $\alpha_0 = 55^\circ$ (Fig. 4). The reduced frequency of the models' oscillation in the measuring space of the water tunnel was $f = 0.0197$.

Dynamic tests were conducted for a numbers of values of reduced frequency and over a wide range of angles of attack (see Figs. 5 and 6). The amplitude of changes in the angles of attack was $\Delta\alpha = 5^\circ$ at a basic angle of attack $\alpha_0 = 15^\circ$. Figure 7 shows the effect of the reduced frequency on maximum (C_Z-max, C_m-max) and minimum (C_Z-min, C_m-min) values of the aerodynamic coefficients in the hysteresis loops.

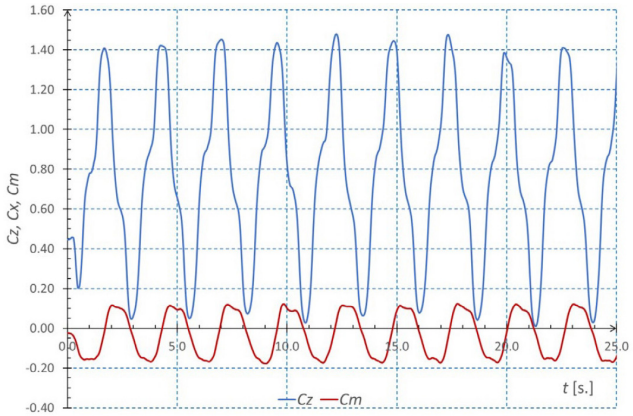

Fig. 3. Waveform of measured unsteady characteristics C_Z, C_m as functions of time, Re = 28 000, $\alpha_0 = 25^\circ$, $\Delta\alpha = 5^\circ$, $f = 0.0197$

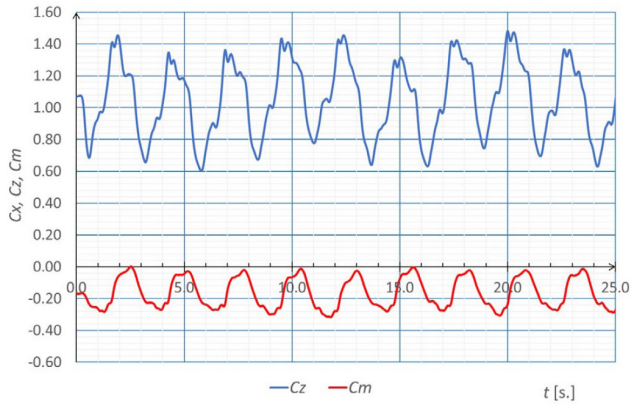

Fig. 4. Waveform of measured unsteady characteristics C_Z, C_m as functions of time, Re = 28 000, $\alpha_0 = 55^\circ$, $\Delta\alpha = 5^\circ$, $f = 0.0197$

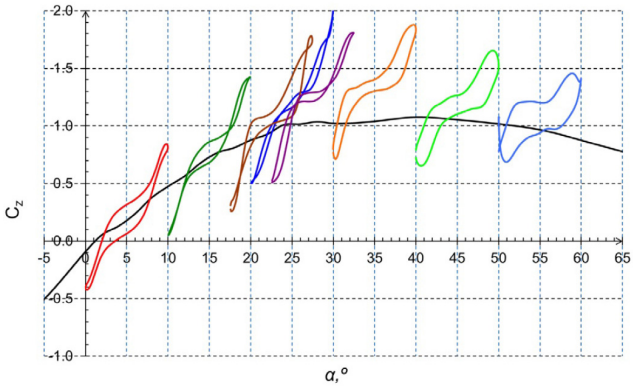

Fig. 5. Static characteristic (black line) and hysteresis (colored lines) of $C_Z(\alpha)$: $f = 0.0197$, Re = 28 000

There is an almost linear relationship between the reduced frequency and the parameters of the hysteresis loops, both for the lift coefficient and the pitching moment coefficient. An increasing of the reduced frequency results in an increase in the distance between the maximum and minimum values of the coefficients in the hysteresis loops.

Unsteady aerodynamics determine the boundaries of the flight envelope of a microdrone. It is also possible to apply an

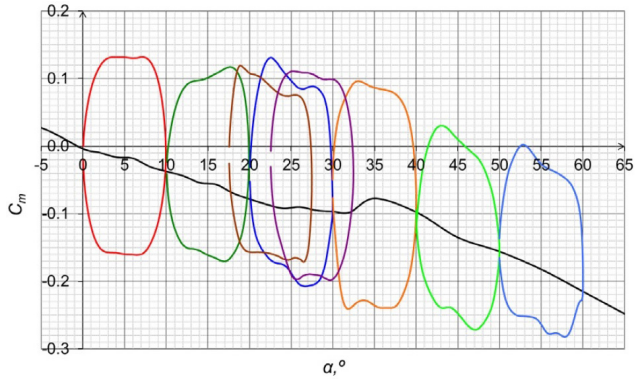

Fig. 6. Static characteristic (black line) and hysteresis (colored lines) of $C_m(\alpha)$: $f = 0.0197$, Re = 28 000

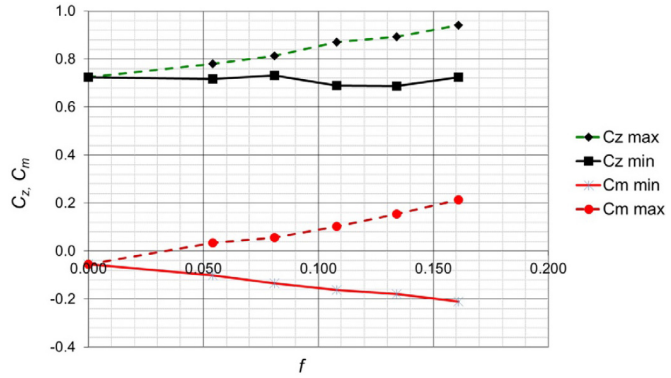

Fig. 7. Maximum and minimum values of lift and pitching moment coefficients as functions of reduced frequency f of oscillations; $\alpha_0 = 15°$, $\Delta\alpha = 5°$, Re = 28 000

artificial neuron network (ANN) for modelling unsteady aerodynamics of an s-wMAV. In the literature, ANN architectures suitable for modeling of the unsteady aerodynamic characteristics in the extended angle-of-attack range have been discussed. It can also be noticed that a considerable number of papers contributions discuss the application of ANN in modeling unsteady aerodynamics of jet fighters or the new generation of passenger airliners [7, 11–17].

The results of the experimental data simulation using the neural network model are presented below.

3. NEURAL NETWORK

The essence behind the operation of a network is the fact that individual neurons are interconnected via links, which are the equivalent of synaptic bonds [18]]. The so-called weights of the links are modified in a network. Network training is about changing link weights. Information stored within a network is of distributed character, i.e. it is almost impossible to determine which network fragment reflects which of its features. The consequence is a very interesting property of neural networks – relatively high resistance to damage. Information processing power within a neural network stems from the fact that individual neurons can simultaneously process information. Because neuron outputs within a given layer depend solely on the neuron outputs of the previous layer, i.e. neurons in each layer are independent, it is possible to apply simultaneous signal processing. Individual network layers can also execute simultaneous calculations, transferring their results inside the network in cycles. Therefore, information is processed in a streamline. Response to an output signal appears at the output after n cycles. However, because a network simultaneously processes n consecutive excitations, one per each layer, it is possible to conduct calculations with a frequency equal to information transfer between neural network layers.

The model by McCulloch and Pitts, formulated in 1943, was one of the first neuron models [19, 20]. Neuron was adopted as a binary unit. The electrical diagram of this model is shown in Fig. 8.

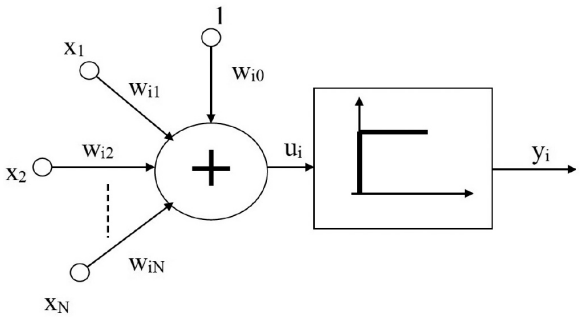

Fig. 8. Artificial neuron model according to McCulloch and Pitts [19]

Pursuant to the source literature [21], input signals x_j ($j = 1, 2, \ldots, N$) are added with appropriate weights w_{ij} in an adder, and then compared with the threshold w_{i0}. A neuron output signal y_i is expressed by the following relationship [21]:

$$y_i = f\left(\sum_{i=1}^{N} w_{ij}x_j(t) + w_{i0}\right). \tag{1}$$

The argument of this function is an adder signal:

$$u_i = \sum_{i=1}^{N} w_{ij}x_j(t) + w_{i0} \tag{2}$$

Function $f(u)$ is called the activation function. In the McCulloch-Pitts model, this is a step function described by the following relationship [18–21]:

$$f(u) = \begin{cases} 1, & u > 0, \\ 0, & u \leq 0. \end{cases} \tag{3}$$

Coefficients w_{ij} represent the weights of synaptic connections. A positive value of these coefficients means an excitation synapse, negative means an inhibitory one. The McCulloch-Pitts is a discrete model, where the neuron state at moment $(t+1)$ is determined based on the state of neuron input signals at the previous moment t. Adopting a discrete model is justified by the presence of the phenomenon of refraction only in a real nerve cell, which causes a neuron to be able to change its state with a certain limited frequency, and with the presence of dead zones.

Functions more useful in terms of modelling artificial neural networks are sigmoidal functions, since they are continuous, which facilitates the training process.

A sigmoidal neuron exhibits a structure similar to the McCulloch-Pitts model. However, it differs in that the activation function is continuous. This study utilized a bipolar sigmoidal function [21,22], which can be expressed as:

$$f(x) = \tanh(\beta x). \tag{4}$$

Coefficient β is a parameter selected by the user. Its value impacts the shape of the activation function. Sample waveforms of the bipolar sigmoidal function relative to variable x for various parameters β are shown in Fig. 9.

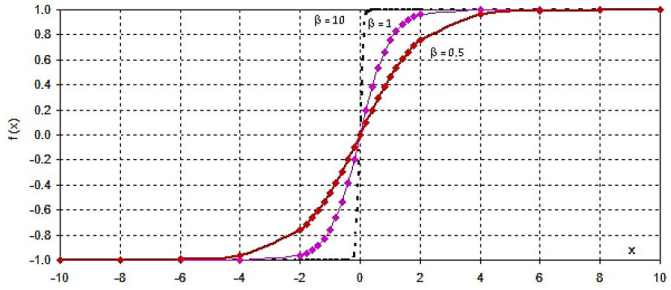

Fig. 9. Sample waveforms of bipolar sigmoidal function [21]

As seen in the image above, at low values of β, the activation function has a mild waveform, while its steepness increases with the increasing value of β. The value of this coefficient, for the purposes of calculations in this elaboration, was adopted at 0.5. The differentiability of the bipolar sigmoidal function is its key feature. This property can be used for neural network training by means of applying the gradient method. To put it simply, it is a steepest descent method [21,22], according to which the weights are updated:

$$w = [w_{i0},\ w_{i1},\ \ldots,\ w_{iN}]^T \tag{5}$$

towards a negative gradient of the shape objective function

$$E = \frac{1}{2}(y_i - d_i)^2 \tag{6}$$

where:

$$y_i = f\left(\sum_{j=1}^{N} w_{ij} \cdot x_j\right) \tag{7}$$

whereby y_i is the current output value of the i-th neuron.

In relationship (6), the j gradient component has the form below:

$$\nabla jE = \frac{\partial E}{\partial w_{ij}} = e_i x_j \frac{df(u_i)}{du_i} \tag{8}$$

where: $e_i = (y_i - d_i)$ – difference between the neuron signal output value and the set value.

By adopting the designation:

$$\delta_i = e_i \frac{df(u_i)}{du_i} \tag{9}$$

we can determine the j gradient component in the form of

$$\nabla_j E = \delta_i x_j. \tag{10}$$

Weights can be updated discretely, in accordance with:

$$w_{ij}(t+1) = w_{ij}(t) - \eta \delta_i x_j \tag{11}$$

where η is the training coefficient, usually taken from a range of $(0,1)$ or continuously, by solving a differential equation:

$$\frac{dw_{ij}}{dt} = -\eta \delta_i x_j. \tag{12}$$

The gradient method allows for the determination of only the local minimum, which can be different from a global minimum.

A certain general aid is the application of training with a so-called *momentum* [22]. In this method, the weight update process takes into account not only information on the function gradient, but also the current weight change trend. Mathematically, this method can be represented in the following form:

$$\Delta w_{ij}(t+1) = -\eta \delta_i x_j + \alpha \Delta w_{ij}(t) \tag{13}$$

where: a is the momentum coefficient usually adopted from the range of $(0,1)$.

The first term of formula (13) corresponds to the steepest descent method, while the second component (*momentum*) includes only the last weight change, regardless of the current gradient value. Based on the analyses of the source literature data [23–25], and the ones discussed in this article, it can be concluded that the value of this coefficient, including the component resulting from the *momentum*, has a greater influence on weight selection. Its impact increases significantly near a local minimum, where the gradient value is close to zero. Therefore, in this case, weight changes are possible, which leads to increasing objective function value (6), hence, overcoming the barrier restricting the local minimum. It should be stressed that the *momentum* factor cannot fully dominate the training process, since this would lead to training process instability. Usually the e_i error value is regulated within the training process, allowing for its growth only to a certain extent, e.g. by 10%. In such a case, if $e_i(t+1) < 1.1e_i(t)$, the training step is accepted and the weight values are updated, whereas if $e_i(t+1) \geq 1.1e_i(t)$, the changes are ignored. It is then assumed that $\Delta w_{ij}(t) = 0$ and the gradient component regains dominance over the *momentum* component.

4. NEURAL NETWORK TRAINING METHODS

Each neural network must be subjected to a training process [26–29]. As a result of the training process, a network acquires the ability to independently select the values of weight factors. This ability enables neural networks to independently adapt to changing operating conditions. The objective of neural network training is the appropriate weight selection. Distinguished neural network training methods include training under supervision, training with a critic and self-organizing training.

In the first method, input signals are accompanied by desired values of input signals. The values of weight factors are selected so as to minimize network error, that is, the difference between the value selected by the network and the set output signal values. In subsequent training cycles, the network selects the weight so that its responses are as consistent with the training patterns as possible. A significant feature of this process

is the presence of feedback, which allows for network weight correlation.

The method of training with a critic differs from the previous method in that it does not contain information on required output values, but instead information on whether the results obtained by the network are satisfactory or not. If an operation provides a positive result, the tendency of a system to properly behave in the future, and vice versa, strengthens.

The self-organizing training method involves rivalry between individual neurons for active participation in the training method. Only one neuron can be active in the course of training. Other neurons remain at rest. A group of competing neurons receives the same input signal vectors. Depending on the values of synaptic weights of individual neurons, their output signals differ. The neuron with the highest output value is the winner. It adopts a value of 1 at its output, with the other neurons adopting the value of 0. The winning neuron gains the right to update its weights, namely, the right to continue training.

The general form of the adopted model is shown in Fig. 10. A neural network is a mathematical model, which enables determining the output values n_{st} (coefficients of aerodynamic forces and moments) based on set input signal values of conducted experiments p_{st}.

Fig. 10. Diagram of a mathematical model using neural networks, where [40]: p_s – input signal vector; p'_{st} is the standardized input signal vector; n'_{st} is the standardized output signal vector; n_{st} is the output signal vector, NN is the neural network and A and B are signal transformation matrices

Input signals are the measured values of angular positions of the studied model in the Reynolds number function, reduced motion frequencies of the model and relative propeller advance at set values of the angular position in relation to other reference planes. Measured values of the aerodynamic coefficients specific for a given motion plane are used as training values.

In the general case, output parameters are an input parameter function. A one-way, multi-layered perceptron network with sigmoidal neurons was used to determine a mathematical model of the initial parameter and aerodynamic coefficient vector [22]. The structure of the utilized network is shown in Fig. 11.

The method with a trainer, utilizing experimental results, was applied for network training. It involved applying the perceptron rule [19, 27–33], according to which the weights are selected within a cycle using the momentum error back propagation algorithm [27, 28], which determines the strategy of weight selection in a multi-layered network, using gradient optimization methods. According to this method, network training consists of several stages. The first stage involves the presentation of a training sample **x** and calculating the values of signals for individual neurons within the network. The values of the hidden layer neuron output signals, followed by the y_i values, corresponding to the output layer neurons, are calculated for a given vector **x**. The second stage involves minimizing the function objective. Under the assumption of the continuity of this function, the gradient optimization methods remain the most effective training methods [21]. According to this general pattern, three stages are distinguished within each training cycle. The first one is the analysis of a neural network with typical signal flow direction, under the assumption of network input signals equal to the elements of the current vector **x**. The analysis outcome are the values of output signals for the neurons of hidden layers and the output layer, as well as appropriate derivatives of the activation function in individual layers. The second one involves creating a back-propagation network by reversing the signal flow direction, replacing the activation function by their derivatives, as well as applying an input network at the former output (currently input), in the form of an appropriate difference between the current and set values. The values of appropriate back differences shall be calculated for such a network. The third stage includes weight adaptation based on the results of the two previous stages. This process should be repeated for all training patterns, until the gradient standard falls below a certain value, which determines the training process accuracy.

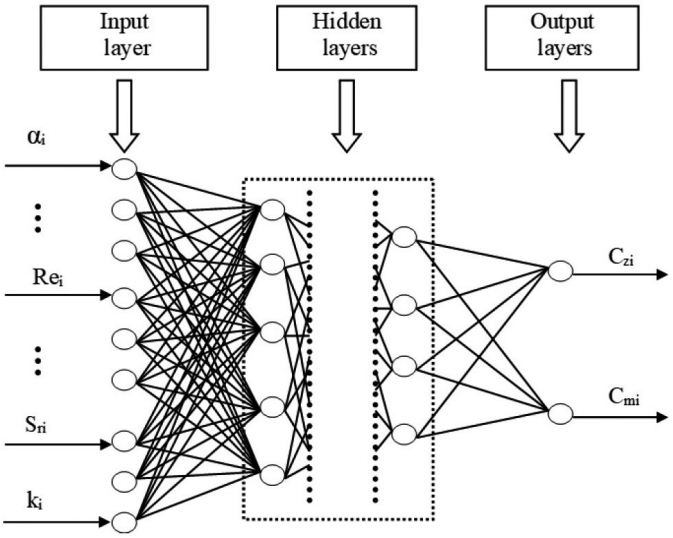

Fig. 11. Neural network structure

For the analysis of the mathematical model, a unidirectional multilayer perceptron network with sigmoid neurons was used. The neural network undergoes a learning process. The purpose of learning is to select the weights of the neural network in such a way that it simultaneously generates all the parameters necessary to implement the model with an acceptable error level. The selection of synaptic weights takes place in a cycle that uses the algorithm of the instantaneous error back propagation method, which defines the strategy of selecting weights in a multilayer network using gradient optimization methods. The authors' computer program SSN JETNETT 2.0 was used for teaching neural networks. The designed neural network, after having learned, should be tested in order to assess the accuracy of mapping the real object by the neural network. The determination of its use for simulation studies is based on the test results [30].

Below you can find the neural network training results for various network structures (number of layers, number of neurons in the layers, input and output parameter structures). Ex-

perimental data were used for neural network training in order to generate aerodynamic parameters C_Z and C_m. Data in standardized form for neural network training were developed. The applied models were characterized by diverse structures.

Exceeding this parameter resulted in further continuation of the neural network training process and, in consequence, led to a proper selection of synaptic weights (w_i). For instance, in the case of a global test result for a test number of events $l_{pst} = 1000$, the obtained average value χ^2_{avr} was equal to 0.72360E-03, for a tolerance level equal to 0.01. This means that a neural network is a "fast learner". The results of aerodynamic characteristics within the s-wMAV pitch plane, for a Reynolds number of 28 000, identified with neural networks, are shown in Figs. 12 and 13, which present the waveforms for coefficients C_Z and C_m in the function of angle α, for measurements conducted with deactivated propulsion, and the neural network structure in the form of $4 \times 8 \times 8 \times 2$ – four input layer neurons, two eight-neuron hidden layers and a two-neuron output layer. Figures 14 and 15 show waveforms for a neural network with a $3 \times 9 \times 9 \times 2$ structure – three input layer neurons, two nine-neuron hidden layers and a two-neuron output layer; whereas Figs. 16 and 17 show the waveforms for a neural network with a $3 \times 10 \times 9 \times 2$ structure – three input layer neurons, two ten-neuron hidden layers and two output layer neurons.

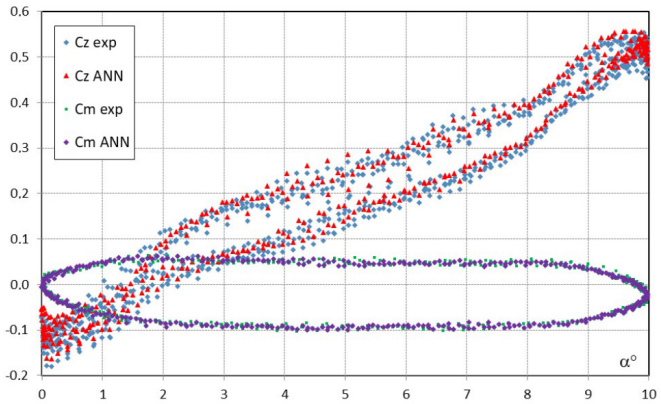

Fig. 12. Waveforms of measured and identified aerodynamic coefficients $C_Z = f(\alpha)$; $C_m = f(\alpha)$, $f = 0.0054$; Re = 28 000; for C_Z $\chi^2_{\text{avr}} = 0.000298$, and for C_m $\chi^2_{\text{avr}} = 2.88\text{E}{-}06$

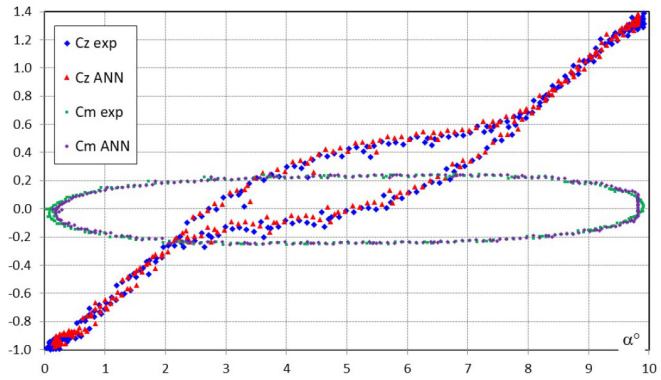

Fig. 13. Waveforms of measured and identified aerodynamic coefficients $C_Z = f(\alpha)$; $C_m = f(\alpha)$, $f = 0.0296$, Re = 28 000; for C_Z $\chi^2_{\text{avr}} = 0.001504$, and for C_m $\chi^2_{\text{avr}} = 2.42\text{E}{-}05$

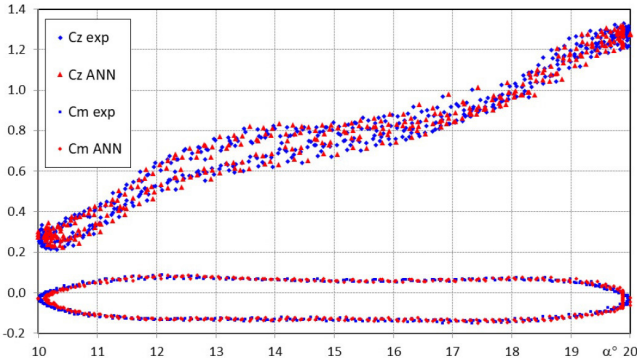

Fig. 14. Waveforms of measured and identified aerodynamic coefficients $C_Z = f(\alpha)$; $C_m = f(\alpha)$, $f = 0.0148$, Re = 28 000; for C_Z $\chi^2_{\text{avr}} = 0.000124$, and for C_m $\chi^2_{\text{avr}} = 5.83\text{E}{-}06$

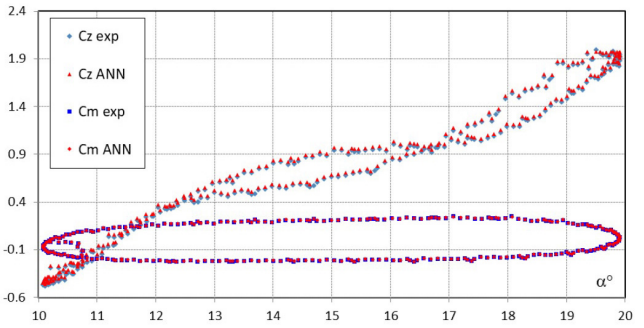

Fig. 15. Waveforms of measured and identified aerodynamic coefficients $C_Z = f(\alpha)$; $C_m = f(\alpha)$, $f = 0.0197$, Re = 28 000; for C_Z $\chi^2_{\text{avr}} = 0.000272$, and for C_m $\chi^2_{\text{avr}} = 1.07\text{E}{-}05$

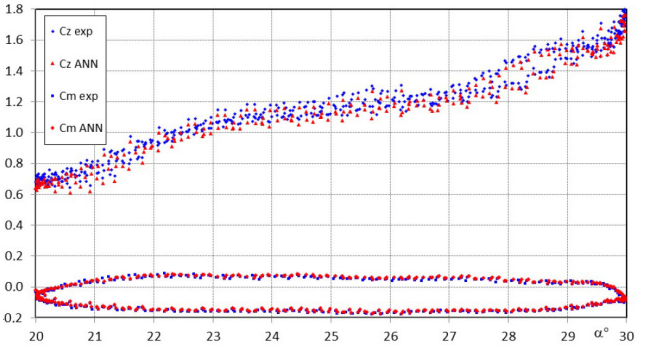

Fig. 16. Waveforms of measured and identified aerodynamic coefficients $C_Z = f(\alpha)$; $C_m = f(\alpha)$, $f = 0.0148$, Re = 28 000; for C_Z $\chi^2_{\text{avr}} = 0.001112$, and for C_m $\chi^2_{\text{avr}} = 5.86\text{E}{-}5$

The selection of neural training coefficients, training constant η and the *momentum* parameter played an important role in the training process. They impact the training process speed and the increment of weight value changes in the course of the neural training process. A too low *momentum* parameter value significantly slows down the training process, however it enables avoiding the so-called generalization error and reaching a global minimum of the objective function. Whereas too high values of these parameters, i.e. those close to 1, significantly impact the value of the error determined with equation (14) and the obtained output parameter values exceed the assumed

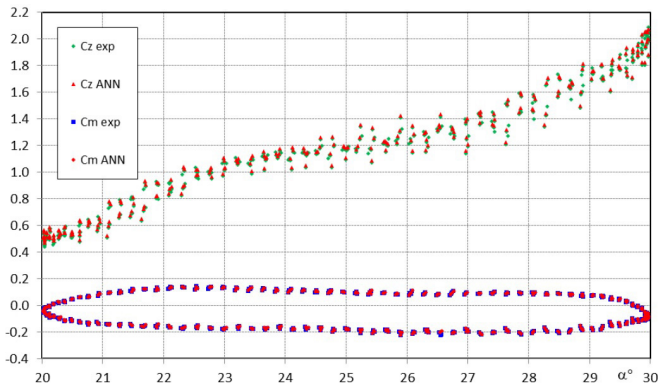

Fig. 17. Waveforms of measured and identified aerodynamic coefficients $C_Z = f(\alpha)$; $C_m = f(\alpha)$, $f = 0.0197$, Re = 28 000; for C_Z $\chi^2_{\text{avr}} = 0.000272$, and for C_m $\chi^2_{\text{avr}} = 1.70\text{E}{-5}$

permissible error level. One of the fundamental properties of neural networks is the ability to generalize the knowledge acquired.

A network trained on a training data set generates expected results when its input is subjected to a set of data belonging to this group, yet not participating in the training process. Selecting synaptic weights of a network within a training process is aimed at shaping its properties, so that it reproduces the sequence of set training pairs as best as possible. A neural network should acquire the ability to generalize, so that based on weight coefficients generated within the training process, it is able to generate output data for input parameters different from the ones used in the training process, thus obtaining the ability to generalize, apart from reproductive capabilities. In order for a neural network to acquire good generalization capabilities, it must be trained on a redundant set, because only then can the weights adapt not to individual data, but to their statistical representation. Hence, one should act with the aim to minimize a network's structure, as well as operate on a sufficiently large set of training data, in order to obtain good network generalization. The ultimate decision in terms of selecting the final network form can be made only following full training of numerous structures.

5. CONCLUSIONS

Identification with the use of neural networks allows for mapping measurement results with an accuracy in the order of 1%. As a result, a correctly trained neural network can be used to obtain characteristics for other (as compared with the ones obtained based on aerodynamic tunnel tests) reduced model motion frequencies, reduced propeller frequency, different Reynolds number or a wide range of angles of attack. However, please note that a short-term oscillatory motion performed by an s-wMAV model during experimental tests does not directly reflect any actual maneuver but only the flow specificity during a dynamic motion, within a selected range of angular positions and for specified similarity numbers [2, 3, 6, 15, 16]. The objective of the experiments was to acquire data for the identification of s-wMAV aerodynamic loads, and in this regard, the very use of a mathematical relationship for describing thus measured discredited values, with an accuracy of 10%, can be considered sufficient.

Based on the analysis of the water tunnel test results, it can be concluded that reliable aerodynamic characteristics of the micro-aircraft were obtained both in stationary as well as nonstationary conditions. The research also involved the determination of aerodynamic characteristics for a wide range of angular positions of the studied s-wMAV model [2, 3]. In the case of dynamic tests, reduced frequency of the short-term oscillatory motion is the similarity criterion most important from the perspective of mapping aircraft motion in under disturbed atmosphere. It seems that this parameter is more paramount than the Reynolds number, since it relates directly to the non-stationarity of the flow caused by the motion performed by an actual object when flying in a turbulent atmosphere. The range of reduced frequencies for the Reynolds numbers assumed was selected based on the analysis of the "Bee" s-wMAV in-flight tests records [1, 3]. During the non-stationary water tunnel tests, the range of angular velocities of the model's motion, after converting relative to the flight conditions of the "Bee" micro-aircraft in the atmosphere, was from 0.5 [1/s] to 2 [1/s] [2, 3]. The tests also involved a broad range of angles of attack, going far beyond the critical parameters. The influence of a rotating propeller in a leading-edge extension on the aerodynamic characteristics of an s-wMAV was also studied, taking into account the similarity criterion – advance ratio and the Strouhal number. A positive impact of the slipstream on wing flow, especially for flow at a lower Reynolds number, was demonstrated [2, 3].

Micro aerial vehicles are a relatively new class of unmanned aerial vehicles. The experimental tests of objects in this class are currently conducted at many research centers [35–40]. The aerodynamic characteristics of micro-aircraft are obtained by way of CFD simulation [1, 39–41], wind or water tunnels testing [1–3, 13, 17, 18, 35–39], or by way of in-flight tests [42, 43]. Most publications concern the issue of measuring stationary characteristics, usually within a single plane of micro-aircraft motion, with the objective of such tests being the determination of basic aerodynamic characteristics. The issue of fixed-wing micro-aircraft flight dynamics is approached relatively rarely, and even in this case, the dynamic properties are usually studied relative to a single motion plane, most often the pitch plane [44]. Global source literature rarely addresses the modelling of s-wMAV characteristics using the artificial neural networks approach in the range of low Reynolds numbers.

REFERENCES

[1] C. Galiński and R. Żbikowski, "Some problems of micro air vehicles development," *Bull. Polish Acad. Sci. Tech. Sci*., vol. 55, no. 1, pp. 91–98, 2007.

[2] K. Sibilski, M. Nowakowski, D. Rykaczewski, P. Szczepaniak, A. Żyluk, A. Sibilska-Mroziewicz, M. Garbowski, and W. Wróblewski, "Identification of fixed-wing micro aerial vehicle aerodynamic derivatives from dynamic water tunnel tests," *Aerospace*, vol. 7, no. 8, p. 116, 2020, doi: 10.3390/aerospace7080116.

[3] K. Sibilski, M. Lasek, A. Sibilska-Mroziewicz, and M. Garbowski, *Dynamcs of Flight of Fixed Wings Micro Aerial Vehicles*, Publishing House of the Warsaw University of Technology, Warsaw, 2020.

[4] M. Abdulrahim, S. Watkins, R. Segal, M. Marino, and J. Sheridan, "Dynamic sensitivity to atmospheric turbulence of fixed-wing UAV with varying configuration," *J. Aircaft*, vol. 47, no. 6, pp. 1873–1883, 2010, doi: 10.2514/1.46860.

[5] A.N. Kolmogorov, "On the representation of continuous functions of many variables by superposition of continuous functions of one variable and addition," *Dokl. Akad. Nauk SSSR*, vol. 114, no. 5, pp. 953–956, 1957, [in Russian].

[6] W.E. Faller, S.J. Schreck, and H.E. Helin, "Real-time model of three dimensional dynamic reattachment using neural networks," *J. Aircraft*, vol. 32, no. 6, pp. 1177–1182, 1995, doi: 10.2514/3.46861.

[7] W.F. Faller and S.J. Schreck, "Unsteady fluid mechanics applications of neural networks," *J. Aircraft*, vol. 34, no. 1, pp. 48–55, 1997, doi: 10.2514/2.2134.

[8] M. Kerho and B. Kramer, *Research water tunnels – specification, Rolling Hills Research Corporation (RHRC)*, El Segundo, CA, USA, 2003.

[9] M. Kerho and B. Kramer, *Five-component balance and computer-controlled model support system for water tunnel applications*, Rolling Hills Research Corporation (RHRC), El Segundo, CA, USA, 2009.

[10] M. Kerho and B. Kramer, *Ultrasonic flowmeter and temperature probe, Rolling Hills Research Corporation (RHRC)*, El Segundo, CA, USA, 2010.

[11] P.H. Reisenthel, "Development of nonlinear indicial model using response functions generated by a neural network," in *Proceedings of the 35th Aerospace Sciences Meeting and Exhibit*, Reno, NV, USA, 6–9 January 1997, p. AIAA 97–0337, doi: 10.2514/6.1997-337.

[12] S. Hitzel and D. Zimper, "Wind tunnel simulation and 'Real' flight of advanced combat aircraft: industrial perspective," *J. Aircraft*, vol. 55, no. 2, pp. 587–602, 2018, doi: 10.2514/1.C033696.

[13] D. Rohlf, S. Schmidt, and J. Irving, "Stability and control analysis for an unmanned aircraft configuration using system-identification techniques," *J. Aircraft*, vol. 49, no. 6, pp. 1597–1609, 2012, doi: 10.2514/1.C031392.

[14] D.J. Ignatyev and A.N. Khrabrov, "Neural network modelling of unsteady aerodynamic characteristics at high angles of attack," *Aerospace Sci. Technol*., vol. 41, pp. 106–115, 2015, doi: 10.1016/j.ast.2014.12.017.

[15] D. Ignatyev and A. Khrabrov, "Experimental study and neural network modeling of aerodynamic characteristics of canard aircraft at high angles of attack," *Aerospace*, vol. 5, no. 1, p. 26, 2018, doi: 10.3390/aerospace5010026.

[16] P.C. Murphy, V. Klein, and N.T. Frink, "Nonlinear unsteady aerodynamic modeling using wind-tunnel and computational data," *J. Aircraft*, vol. 54, no. 2, pp. 659–683, 2017, doi: 10.2514/1.C033881.

[17] P. Murphy, V. Klein, and N. Szyba, "Progressive aerodynamic model identification from dynamic water tunnel test of the F-16XL aircraft," in *Proceedings of the AIAA Atmospheric Flight Mechanics Conference and Exhibit, Guidance, Navigation, and Control and Co-located Conferences*, 2004, Providence, RI, USA, p. AIAA 2004–5727, doi: 10.2514/6.2004-5277.

[18] B. Paprocki, A. Pregowska, and J. Szczepański, "Optimizing information processing in brain-inspired neural networks," *Bull. Polish Acad. Sci. Tech. Sci*., vol. 8, no. 2, pp. 225–233, 2020, doi: 10.24425/bpasts.2020.131844.

[19] W.S. McCulloch and W. Pitts, "A logical calculus of the ideas immanent in nervous activity," *Bull. Math. Biophys*., vol. 5, no. 4, pp. 115–133, 1943, doi: 10.1007/BF02478259.

[20] J. Hertz, A. Krogh, and R. Palmer, *Introduction to the theory of neural computation*, CRC Press, Taylor & Francis Inc., London – N-York, 1991.

[21] R.A. Kosiński, *Artificial neural networks. non-linear dynamics and chaos*, PWN, Warszawa, 2017.

[22] S. Osowski, *Neural networks for information processing, 4th Edition*, Publishing House of the Warsaw University of Technology, Warsaw, 2020.

[23] R. Tadeusiewicz, *Neural networks*, Akademic Publisching House, Warsaw, 1993.

[24] K. Diamantaras and S. Kung, *Principal component neural networks, theory and application*, J. Wiley, New York, 1996.

[25] R. Lippmann, "An introduction to computing with neural nets," *IEEE ASSP Mag*., vol. 4, no. 2, pp. 4–22, 1987, doi: 10.1109/MASSP.1987.1165576.

[26] K.S. Narendra and K. Parthasarathy, "Identification and control of dynamical systems using neural network", *IEEE Trans. Neural Networks*, vol. 1, no. 1, pp. 4–27, 1990, doi: 10.1109/72.80202.

[27] A. Cichocki and R. Unbehauen, "Neural networks for solving systems of linear equations and related problems," *IEEE Trans. Circuits Syst. I: Fundam. Theory Appl*., vol. 39, no. 2, pp. 124–138, 1992, doi: 10.1109/81.167018.

[28] J. Denoeux and R. Lengalle, "Initialising back propagation networks with prototypes," *Neural Networks*, vol. 6, no. 3, pp. 351–363, 1993, doi: 10.1016/0893-6080(93)90003-F.

[29] E. Karnin, "A simple procedure for pruning backpropagation trained neural networks," *IEEE Trans. Neural Networks*, vol. 1, no. 2, pp. 239–242, 1990, doi: 10.1109/72.80236.

[30] J. Manerowski and D. Rykaczewski, "Modelling of UAV flight dynamics using perceptron artificial neural networks," *J. Theor. App. Mech*., vol. 43, no. 2, pp. 297–307, 2005.

[31] R. Barron, "Approximation and estimation bounds for artificial neural networks," *Machine Learning*, vol. 14, pp. 115–133, 1994, doi: 10.1007/BF00993164.

[32] J.F. Horn, A.J. Calise, and J.V.R. Prasad, "Flight Envelope Cueing on a Tilt-Rotor Aircraft Using Neural Network Limit Prediction," *J. Amer. Helic. Soc*., vol. 46, no. 1, pp. 23–31, 2001, doi: 10.4050/JAHS.46.23.

[33] T. Cepowski and T. Szelangiewicz, "Application of Artificial Neural Networks to investigations of ship seakeeping ability," *Pol. Marit. Res*., vol. 8, no. 3, pp. 11–15, 2001.

[34] T. Mueller, "Aerodynamic Measurements at Low Reynolds Number for Fixed Wing Micro-Air Vehicles," in *AVT/VKI Special Course on Development and Operation of UAVs for Military and Civil Applications*, NATO/VKI, Brussel, Belgium, 1999.

[35] Dong Sun, Huaiyu Wu, Rong Zhu, and Ling Che Hung, "Development of Micro Air Vehicle Based on Aerodynamic Modeling Analysis in Tunnel Tests," in *Proceedings of the 2005 IEEE International Conference on Robotics and Automation*, Barcelona, Spain, 2005, pp. 2235–2240, doi: 10.1109/ROBOT.2005.1570445.

[36] R. Randall, S. Shkarayev, G. Abate, and J. Babcock, "Longitudinal aerodynamics of rapidly pitching fixed-wing Micro Air Vehicles," *J. Aircraft*, vol. 49, no. 2, pp. 453–471, 2012, doi: 10.2514/1.C031378.

[37] C. Tongchitpakdee, W. Hlusriyakul, C. Pattanathummasid, and C. Thipyopas, "Aerodynamic investigation and analysis of wingtip thickness's effect on low aspect ratio wing," in *Proc. International Micro Air Vehicle Conference and Flight Competition (IMAV2013)*, Toulouse, France, 2013.

[38] J-M. Moschetta, "The aerodynamics of micro air vehicles: technical challenges and scientific issues," *Int. J. Eng. Sys. Model. Sim*., vol. 6, no. 3/4, pp. 134–148, 2014, doi: 10.1504/IJESMS.2014.063122.

[39] D. Viieru, J. Tang, Y. Lian, H. Liu, and W. Shy, "Flapping and flexible wing aerodynamics of low Reynolds number flight vehicles," in *Proc. 44th AIAA Aerospace Sciences Meeting and Exhibit*, Reno, NV, USA, 2006, p. AIAA 2006–503, doi: 10.2514/6.2006-503.

[40] D. Gyllhem, K. Mohseni, and D. Lawrence, "Numerical simulation of flow around the Colorado Micro Aerial Vehicle," in *Proceedings 35th AIAA Fluid Dynamics Conference and Exhibit*, Toronto, Canada, 2005, p. AIAA 2005–4757, doi: 10.2514/6.2005-4757.

[41] V.V. Golubev and M,R. Visbal, "Modeling MAV response in gusty urban environment," *Int. J. Micro Air Veh*., vol. 4, no. 1, pp. 79–92, 2012, doi: 10.1260/1756-8293.4.1.79.

[42] R. Cory and R. Tedrake, "Experiments in fixed-wing UAV perching," in *Proceedings AIAA Guidance, Navigation and Control Conference and Exhibit*, Honolulu, Hi, USA, 2008, p. AIAA 2008–7256, doi: 10.2514/6.2008-7256.

[43] D.V. Uhlig and M.S. Selig, "Stability characteristics of Micro Air Vehicles from experimental measurements," in *Proc. 29th AIAA Applied Aerodynamics Conference*, Honolulu, HI, USA, 2011, p. AIAA 2011–3659. doi: 10.2514/6.2011-3659.